European Cells and Materials Vol. 31 2016 (pages 79-94) DOI: 10.22203/eCM.v031a06 ISSN 1473-2262

CHONDROGENESIS OF MESENCHYMAL STEM CELLS IN A NOVEL HYALURONATE-COLLAGEN-TRICALCIUM PHOSPHATE SCAFFOLDS FOR KNEE REPAIR

F.G. Meng[§], Z.Q. Zhang[§], G.X. Huang, W.S. Chen, Z.J. Zhang, A.S. He and W.M. Liao*

Department of Joint Surgery, First Affiliated Hospital of Sun Yat-sen University, Guangzhou, Guangdong 510080, China

[§]These two authors contributed equally to this work.

Abstract

Scaffolds are expected to play a key role in the induction of chondrogenesis of mesenchymal stem cells (MSCs) for cartilage tissue regeneration. Here, we report the development of a novel tricalcium phosphate-collagen-hyaluronate (TCP-COL-HA) scaffold that can function as a stem cell carrier to induce chondrogenesis and promote cartilage repair, and the investigation of chondroinductive properties of scaffolds containing varying amounts of TCP, COL and HA. TCP-COL-HA scaffolds, as well as TCP-COL scaffolds at two different TCP/COL ratios (50:50 and 25:75), were evaluated for their ability to induce cartilage regeneration from rabbit mesenchymal stem cells (rMSCs) *in vitro* and *in vivo*. Chondrogenic differentiation was evaluated by sulphated glycosaminoglycan quantification, collagen type II immunohistochemistry, and qRT-PCR. Mechanical strength was evaluated by the compression test. The results showed that the TCP-COL-HA scaffolds enhanced rMSC chondrogenesis to a greater degree than did the TCP-COL scaffolds; for the latter, the scaffold with the lower TCP/COL ratio (25:75) was superior in terms of promoting rMSC chondrogenesis. Similar results were obtained in an ectopic implantation model in nude mice. In a critical-size rabbit osteochondral defect-repair model, rMSCs seeded on TCP-COL-HA scaffolds showed greater cartilage regeneration and integration into surrounding tissue than the TCP-COL groups, in which cartilage repair was more efficient at the 25:75 than at the 50:50 ratio. These results indicate that the addition of HA and different TCP/COL ratios can affect the chondroinductive capacity of scaffolds, and suggest that the TCP-COL-HA scaffold can serve as an effective cell carrier for cartilage regeneration.

Keywords: Cartilage engineering, mesenchymal stem cell, hyaluronic acid, collagen, biomaterial, chondrogenesis.

*Address for correspondence:
Dr. Weiming Liao, MD, PhD
Department of Orthopaedic Surgery
First Affiliated Hospital of Sun Yat-sen University
#58 Zhongshan 2nd Road
Guangzhou 510080, China
Telephone Number: 86-20-8775-5766
FAX Number: 86-20-8733-2150
E-mail: liaowmsysu@163.com

Introduction

Damaged articular cartilage has poor self-repair capability owing to the low metabolic rate of chondrocytes (Chen *et al*., 2009; Hunziker, 2002; Steadman *et al*., 2002). Tissue engineering is considered a potential strategy for regenerating damaged tissue (Jackson and Simon, 1999). Mesenchymal stem cells (MSCs) are an especially promising tool since they can be easily isolated from bone marrow and expanded *in vitro* without the loss of their capacity to differentiate into various cell types, including chondrocytes and osteoblasts (Caplan, 2005).

Scaffolds also play critical roles in tissue regeneration (Langer and Vacanti, 1993), as they provide cells with a structural basis for growth and facilitate cellular activities such as proliferation and differentiation that are required for tissue repair (Hubbell, 2003). Scaffolds consisting of components found in the cellular environment are widely used in tissue engineering because of their excellent biocompatibility. Hyaluronan (HA) and collagen (COL) are both key components of the extracellular matrix (ECM) of normal articular cartilage, which provides a favourable environment for MSC chondrogenesis (Schagemann *et al*., 2013). Owing to its greater availability, type I COL (COLI) has often been used in engineering tissue scaffolds (Glowacki and Mizuno, 2008; Gotterbarm *et al*., 2006). COLI is highly biocompatible, weakly immunogenic, and provides an excellent substrate for cell attachment, migration, proliferation and differentiation (Revell and Athanasiou, 2009). COLI has demonstrated chondro-inductive activity (Kuroda *et al*., 2007; Zhang *et al*., 2012; Zheng *et al*., 2009). However, COL products have relatively poor physical properties, including a lack of wet tensile strength, which is important because scaffolds should be designed to serve a space-filling function in a fluid environment (Bakoš *et al*., 1999). Tricalcium phosphate (TCP) has good biocompatibility and biodegradability and has been shown to improve the mechanical properties of COL scaffolds (Arahira and Todo, 2014; Tanaka *et al*., 2005), as well as having been used in scaffolds for osteochondral regeneration (Ahn *et al*., 2009; Marquass *et al*., 2010; Seo *et al*., 2013; Tanaka *et al*., 2005). Moreover, the Food and Drug Administration have approved several COL-calcium phosphate materials, such as HealosVR (Depuy), CollagraftVR (Zimmer), OssimendVR (Collagen Matrix), and MozaikVR (Integra LifeSciences), for use as a bone-void filler along with bone-marrow extract, which confirm their clinical applicability.

HA is a linear polysaccharide that occurs naturally in articular cartilage and synovial fluid and has been shown

to influence many processes involving the ECM, including matrix formation, cell proliferation and migration, and embryonic tissue development (Goodstone *et al*., 2004). HA-based scaffolds are well tolerated, safe and allow faster cell infiltration – leading to more rapid tissue formation in articular cartilage defect repair (Radice *et al*., 2000; Solchaga *et al*., 2005). Photocrosslinkable HA promotes the retention of the chondrocytic phenotype as well as cartilage matrix synthesis, and accelerates healing in an osteochondral defect model (Nettles *et al*., 2004), whereas a fibrin/HA composite gel efficiently promoted chondrogenic differentiation of MSCs (Park *et al*., 2011). Therefore, HA-based scaffolds have potential therapeutic applications in the treatment of cartilage lesions (Pavesio *et al*., 2003).

Exogenous chondrogenic growth factors are routinely used, but have safety issues over the long term (Curran *et al*., 2006; Mueller *et al*., 2010; Stoop, 2008). For instance, direct injection of transforming growth factor (TGF)-β resulted in side effects on the joints, including osteophytes formation, swelling and synovial hyperplasia (Curran *et al*., 2006; van Beuningen *et al*., 1998). Theoretically, the scaffold material itself could be used to induce chondrogenesis in MSCs; however, studies of chondro-conductive scaffolds are rare. In a previous study, we showed that a TCP-COL-HA scaffold can induce the chondrogenic differentiation of human mesenchymal stem cells (hMSCs) independent of TGF-β *in vitro* (Meng *et al*., 2014). In the present study, we further improved the scaffold and examined its potential for inducing chondrogenic differentiation in MSCs to repair cartilage defect. As a control, we also synthesised scaffolds that were of two different TCP:COL ratios. The aim of this study is to report the further development of a novel TCP-COL-HA scaffold that can function as a stem cell carrier to induce chondrogenesis and promote cartilage repair, and to investigate the chondroinductive properties of scaffolds containing varying amounts of TCP, COL, and HA. We hypothesised that a novel TCP-COL-HA scaffold could function as a stem cell carrier to induce chondrogenesis and thereby promote cartilage repair; its effectiveness as an MSC carrier was investigated by assessing cartilage generation *in vitro* and in nude mouse and rabbit models.

Materials and Methods

Scaffold synthesis

Porous scaffolds were generated by freeze-drying followed by chemical cross-linking. For TCP-COL-HA scaffolds, HA (2 wt%) in dry powdered form and TCP (25 wt%) (both from Sigma, St. Louis, MO, USA) were added to a pure COLI solution (calf; Chuanger Ltd, Taijing, China) (73 wt%). For 50:50 (TCP: 50 wt%, COL: 50 wt%) and 25:75 (TCP: 25 wt%, COL: 75 wt%) control scaffolds, only TCP was added to the COLI solution. After vigorous stirring, solutions were poured into moulds and frozen at −60 °C for about 4 h, followed by lyophilisation for 24 h in a freeze-dryer. Scaffolds were washed three times with 0.001 M sodium bicarbonate solution and then crosslinked with 0.1 M 1-ethyl-3-(3-dimethylaminopropyl) carbodiimide/N-hydroxysuccinimide solution at 4 °C for 12 h. After neutralisation with 0.1 M glycine solution and washes with deionised water, lyophilisation was carried out over 24 h to generate the final scaffolds, which were cut into columns (height × diameter, 7.0 × 3.5 mm) and sterilised with ethylene oxide.

Isolation and culture of rabbit MSCs (rMSCs)

Animal experiments were approved by the Ethics Committee of the First Affiliated Hospital of Sun Yat-sen University (IRB: 2014C-028). rMSCs were harvested from the marrow of 8-week-old New Zealand White rabbits (Guangdong Medical Laboratory Animal Center, Guangdong, China) by density gradient centrifugation (Meng *et al*., 2014) and cultured in α Minimal Essential Medium (α-MEM) supplemented with 10 % foetal bovine serum (FBS), 100 U/mL penicillin, and 100 μg/mL streptomycin (all from Gibco, Grand Island, NY, USA) at 37 °C and 5 % CO_2. Passage 3 (P3) cells were used for experiments (Fig. 1).

rMSC differentiation and phenotypic analysis

Cells at passage 2 (2.5×10^6) were collected and cultured by micromass culture in chondrogenic medium consisting of high-glucose Dulbecco's Modified Eagle's Medium (DMEM) supplemented with 10 ng/mL TGF-β1 (R&D Systems, Minneapolis, MN, USA), 1× human insulin/human transferrin/sodium selenite premix, 1 mM sodium pyruvate, 50 ng/mL vitamin C, 100 nM dexamethasone, and 40 μg/mL proline (all from Sigma, St. Louis, MO, USA) for 14 d as previously described (Johnstone *et al*., 1998). For histological analysis, cells were embedded in paraffin and 5-μm sections were stained with alcian blue (Sigma). For osteogenic and adipogenic differentiation, cells were seeded in 6-well plates at a density of 10^3 cells/cm^2 and cultured for 14 d in osteogenic or adipogenic differentiation medium (Meng *et al*., 2014). Cells were stained with alizarin red and oil red O (both from Sigma) to visualise osteocytes and adipocytes, respectively. For cell surface phenotyping, cells at passage 2 were detached and labelled with fluorophore-conjugated mouse anti-rabbit cluster of differentiation CD29, CD44, CD45, CD34 and CD14 antibodies (BD Biosciences, Franklin Lakes, NJ, USA) and analysed by flow cytometry with a FACS Calibur Coulter EPICS Elite system (BD Biosciences) to detect surface antigen expression.

rMSC seeding onto scaffolds and 3-dimensional culture

Scaffolds were soaked in α-MEM, blotted dry, seeded with rMSCs at 2×10^7 cells/mL in 80 μL α-MEM, and placed in a 24-well plate (one scaffold *per* well). After 2 h incubation at 37 °C to allow rMSCs to diffuse into and adhere to the scaffolds, 1 mL of chondrogenic medium without TGF-β1 was slowly added to each well. The culture medium was replaced every 2-3 d.

Cytotoxicity determination

Cytotoxicity of the various scaffolds was assessed using Cell Counting Kit (CCK)-8 (Dojindo, Kumamoto, Japan). rMSCs were seeded on 24-well tissue culture polystyrene (TCPS) plates at a density of 2×10^4 cells/cm^2. Scaffolds

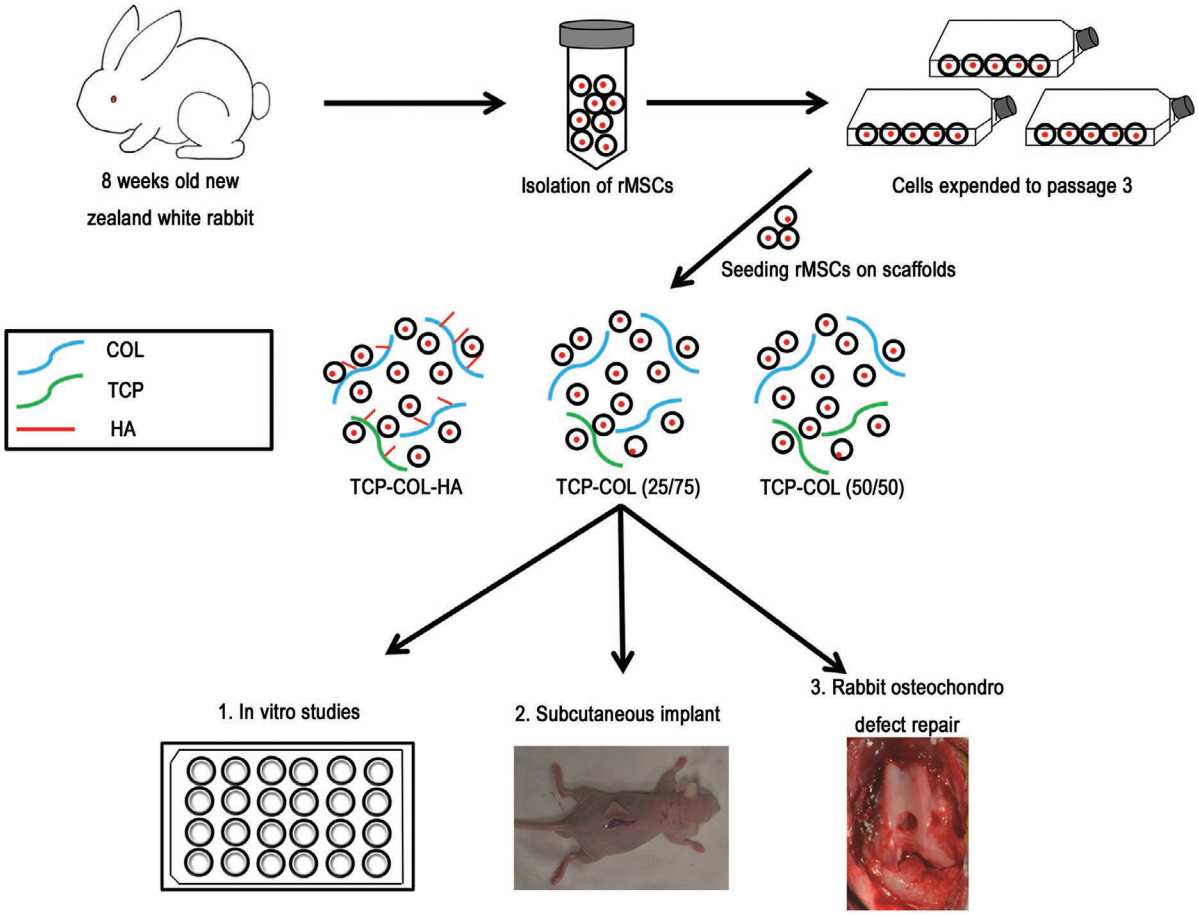

Fig. 1. Schematic illustration of the experimental protocol. rMSCs isolated from rabbit bone marrow were expanded *in vitro*. P3 cells were seeded on TCP-COL-HA, TCP-COL (50:50) and TCP-COL (25:75) scaffolds, which were analysed by *in vitro* assays and *in vivo* models.

were placed onto each well (one scaffold *per* well). rMSCs cultured in wells without scaffolds served as the control group. The rMSCs and scaffolds were cultured at 37 °C in a humidified atmosphere of 5 % CO_2 for 3 and 7 d; the original medium was then replaced with 900 µL DMEM-F12 medium containing 10 % FBS and 100 µL CCK-8 reagent and incubated at 37 °C for 2 h. The supernatant containing water-soluble formazan crystals was transferred to a 96-well plate (100 µL/well), and an optical density (OD) at 450 nm was determined using a Tecan Sunrise microplate reader (Männedorf, Switzerland). Cell viability was normalised to that of cultures in TCPS plates as previously described (Liu *et al*., 2011).

Scanning electron microscopy (SEM) analysis

The morphology of rMSC-seeded scaffolds was examined by SEM. Samples incubated for 3 d and 3 weeks *in vitro* were washed twice with sterile phosphate-buffered saline (PBS, Gibco), fixed in 2.5 % glutaraldehyde for 12 h, dehydrated through a graded series of ethanol for 30 min at each concentration, and critical point-dried. Samples were sputter-coated with gold for 2 min before visualisation by SEM.

Quantitative real-time (qRT-)PCR

Total RNA was extracted using the Total RNA kit (Omega Bio-Tek, Norcross, GA, USA), and 500 ng were reverse-transcribed using the First Strand cDNA Synthesis kit (Takara Bio, Kyoto, Japan). The cDNA served as a template for RT-PCR using SYBR Green (Toyobo Ltd., Osaka, Japan) and the primers listed in Table 1. The relative expression levels of target genes were calculated using the $2^{-\Delta\Delta Ct}$ method by normalising to the level of glyceraldehyde-3-phosphate dehydrogenase. Data were normalised to the TCP-COL (50:50) group, which served as a reference.

Histological analysis

Samples were fixed with 4 % paraformaldehyde (Sigma), decalcified (in the case of samples from the rabbit model), embedded in paraffin, and cut into 5-µm sections that were deparaffinised, rehydrated, and stained with haematoxylin and eosin (H&E) for morphological evaluation and staining with alcian blue and safranin O (both from Sigma) (in the case of samples from the rabbit model) to visualise sulphated glycosaminoglycan (GAG) distribution.

Collagen type II expression was analysed by immunohistochemistry. Sections prepared as described

Table 1. Primers for qRT-PCR.

Genes	Primer sequence (5'→3')	
COLII	Forward	GGCTTTCCTGGAGAGAAAGG
	Reverse	ATAGAACCAGCAGGGCCAGG
Aggrecan	Forward	AGGTCGTGGTGAAAGGTGTTG
	Reverse	GTAGGTTCTCACGCCAGGGA
COLI	Forward	GGCTTTCCTGGAGAGAAAGG
	Reverse	ATAGAACCAGCAGGGCCAGG
COLX	Forward	GAAAACCAGGCTATGGAACC
	Reverse	GCTCCTGTAAGTCCCTGTTGTC
GAPDH	Forward	TCACCATCTTCCAGGAGCGA
	Reverse	CACAATGCCGAAGTGGTCGT
SOX9	Forward	GGTGCTCAAGGGCTACGACT
	Reverse	GGGTGGTCTTTCTTGTGCTG

above were pre-treated with pepsin solution for 15 min at 37 °C and processed with the Envision Detection kit (GeneTech, Shanghai, China) according to the manufacturer's instructions. Briefly, sections were incubated for 10 min with 50 μL 3 % H_2O_2 solution, followed by incubation with mouse anti-rabbit antibody (Abcam, Cambridge, MA, USA) overnight at 4 °C. Negative controls were prepared by substituting PBS for the primary antibody. A biotinylated secondary antibody that was included in the kit was applied for 30 min. Sections were stained with 3,3'-diaminobenzidine tetrahydrochloride (supplied with the kit), counterstained with haematoxylin, dehydrated, and mounted. Immunoreactivity was analysed by determining the integrated optical density (IOD) *per* stained area in μm^2 using Image-Pro Plus 6.0 software (Media Cybernetics, Rockville, MD, USA). Safranin O- and alcian blue-stained areas were also measured using the software.

Biochemical assay for GAG detection

The assay was performed by measuring the reaction between GAGs and dimethylmethylene blue (DMMB) (Sigma). Samples were collected at different time points, washed with PBS, and digested with papain solution for 16 h at 60 °C. A 15-μL aliquot of supernatant was transferred to a new tube and reacted with DMMB solution as previously described (Meng *et al*., 2014). Absorbance was measured at 525 nm. Scaffolds without cells were used as a blank control whose absorbance values were subtracted from those of scaffolds with rMSCs. Total GAG content in each sample was extrapolated using a standard curve obtained with shark chondroitin sulphate (Sigma). To assess the biosynthetic activity of the rMSCs, the results of GAGs quantification were normalised to the dsDNA content. In a 96-well microplate, 100 μL of the extracts were combined with 100 μL of 0.7 μg/mL Hoechst 33258 (Sigma) in water. Fluorescence was read on a GENios Pro™ microplate reader (Tecan, Durham, NC, USA) at excitation and emission wavelengths of 340 and 465 nm, respectively, and was compared to that of a certified calf thymus DNA standard (Amersham Biosciences, Piscataway, NJ, USA).

Analysis of mechanical properties

Cell-seeded scaffolds were subjected to the unconfined compression test using the elf3200 Universal Testing Machine (Bose, Eden Prairie, MN, USA). Tests were performed in displacement control mode at a rate of 3 mm/min. After the test, compressive stress and strain were plotted as a graph based on measured sample dimensions. Peak load was obtained from the load-displacement curve and used to calculate the compressive modulus.

Scaffold implantation in nude mice

Procedures were carried out according to the guidelines of the Ethics Committee of the First Affiliated Hospital of Sun Yat-sen University. Before implantation, P3 rMSCs (2×10^7 cells/mL) were seeded on scaffolds and cultured for 2 weeks in chondrogenic medium without TGF-β1. BALB/c-nude mice (6-8 weeks old; Sun Yat-sen University Laboratory Animal Center, Guangdong, China) were anaesthetised with 1 % sodium pentobarbital in water (1 mL/0.1 kg). A cell-seeded scaffold was subcutaneously implanted into the back of each animal. The incision was closed with sterile sutures and animals were returned to the housing facility where they were allowed to recover and had free access to food and water. After 4 weeks, mice were sacrificed and the scaffolds were collected. Fibrous capsules and other host tissues were carefully removed using fine, straight, toothless forceps, #15 blade in #3 handle under a stereoscope (10× magnification). Scaffolds were rinsed with PBS, and used for biochemical, histological and immunohistochemical analyses.

Rabbit osteochondral defect repair

New Zealand White rabbits (12 knees from 6 rabbits for each group; 16-18 weeks old, weighing 3.0-3.4 kg; Guangdong Medical Laboratory Animal Center, Guangdong, China) were used in this study. rMSC-seeded scaffolds were prepared and cultured in chondrogenic medium without TGF-β1 for 2 weeks prior to implantation. Rabbits were anaesthetised with 5 % sodium pentobarbital (1 mL/kg). The knee was exposed by a medial parapatellar approach and the patella was laterally dislocated. The anterior articular surface of the distal femur was exposed and a 3.3 mm-diameter full-thickness cylindrical osteochondral defect (2-3 mm deep) was made using an electric trephine in the articular surface of the femoral patellar groove. Rabbits were divided into the following groups (n = 6 animals each): control (defect only) or implanted with an rMSC-seeded TCP-COL (50:50), TCP-COL (25:75), or TCP-COL-HA scaffold. Scaffolds were placed in the defect site and the wound was closed by suturing the knee joint capsule and successive layers of the skin. Rabbits were allowed to recover in individual cages. Regenerated tissue/scaffold samples were collected 8 weeks later. Constructs, consisting of regenerated tissue at the original defect sites, as well as surrounding cartilage and bone, were removed from the joints; each sample was cut into two halves, with one used for histological analysis and the other used for biochemical assays and qRT-PCR. For the latter, the regenerated tissue/scaffold sample was carefully and precisely separated from the surrounding native cartilage

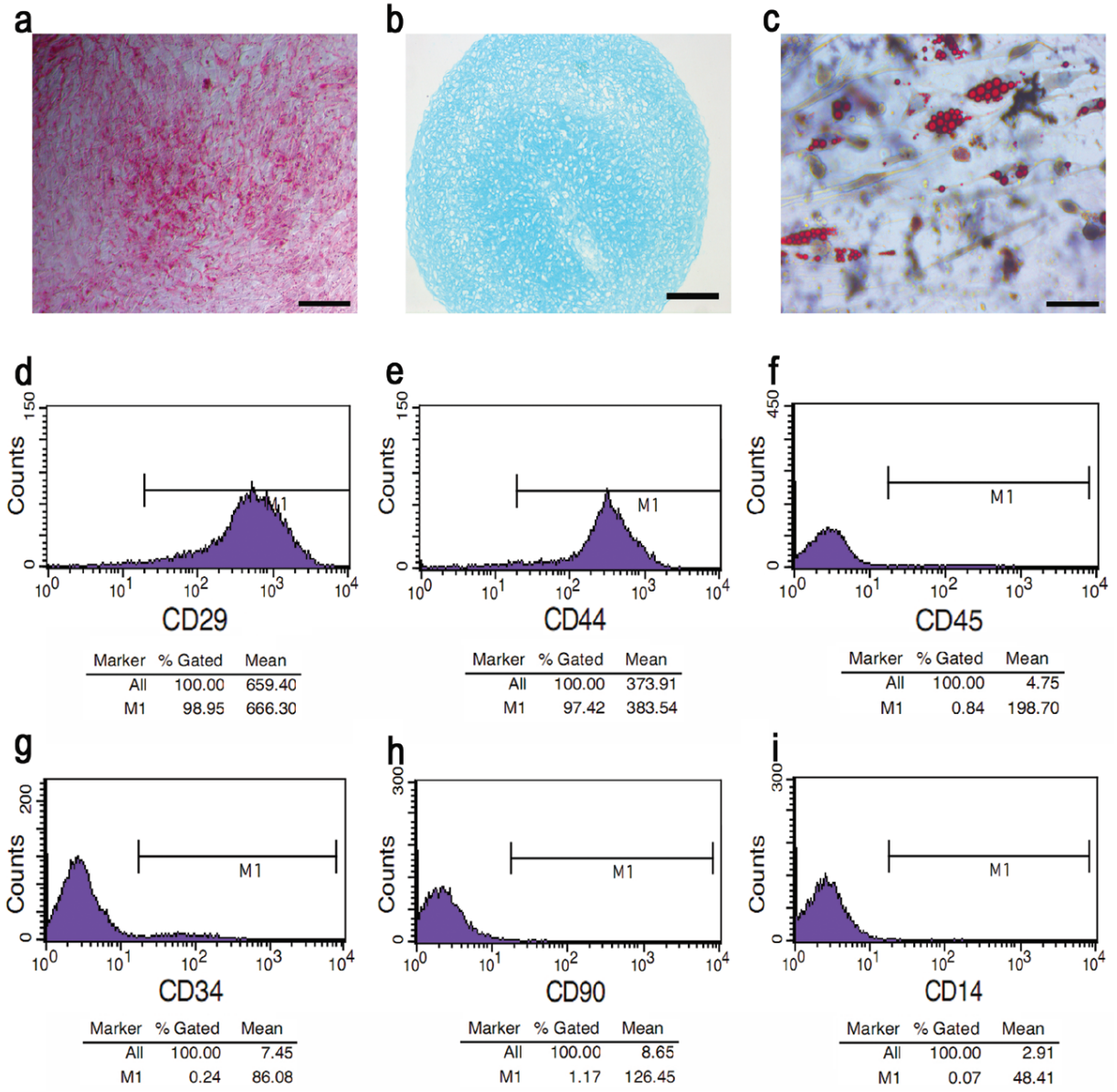

Fig. 2. Trilineage differentiation potential and phenotypic analysis of rMSCs. (**a**) Osteogenic, (**b**) chondrogenic and (**c**) adipogenic differentiation potential were evaluated. (**d-i**) rMSC cell surface antigen characterisation by flow cytometry. The MSC markers CD29 (**d**) and CD44 (**e**) were expressed, while there was no expression of the haematopoietic markers CD45 (**f**), CD34 (**g**), CD90 (**h**) or CD14 (**i**). Scale bar = 200 μm (**a**), 50 μm (**b**, **c**).

and bone using fine, straight, toothless forceps, a #15 surgical scalpel blade in #3 handle under a stereoscope (10x magnification). The regenerated tissue/scaffold was rinsed with PBS and used for the biochemical assay and qRT-PCR.

Statistical analysis

Descriptive statistics were used to assess group means and determine standard deviations from at least three biological replicates. Data were evaluated by one-way analysis of variance (ANOVA) followed by Bonferroni's *post hoc* multiple comparisons test with $p < 0.05$ considered as statistically significant. Analyses were carried out using SPSS v.13.0 for Windows (IBM Corporation, Armonk, NY, USA).

Results

Trilineage differentiation potential and phenotypic analysis

The MSC identity of cells isolated from rabbit bone marrow was confirmed by inducing their differentiation into osteogenic, chondrogenic and adipogenic lineages over 21 d. We also verified the expression of several rabbit MSC markers by flow cytometry. Cells showed positive alizarin red, alcian blue, and oil red O staining (Fig. 2a-c). For the phenotypic analysis, isolated cells at passage 2 were positive for the typical stem cell surface markers CD29 (98.95 %) and CD44 (97.42 %) (Fig. 2d, e), but were negative for the haematopoietic lineage markers CD45, CD34 and CD14 (Fig. 2f-i). These results confirmed that the isolated cells were MSCs.

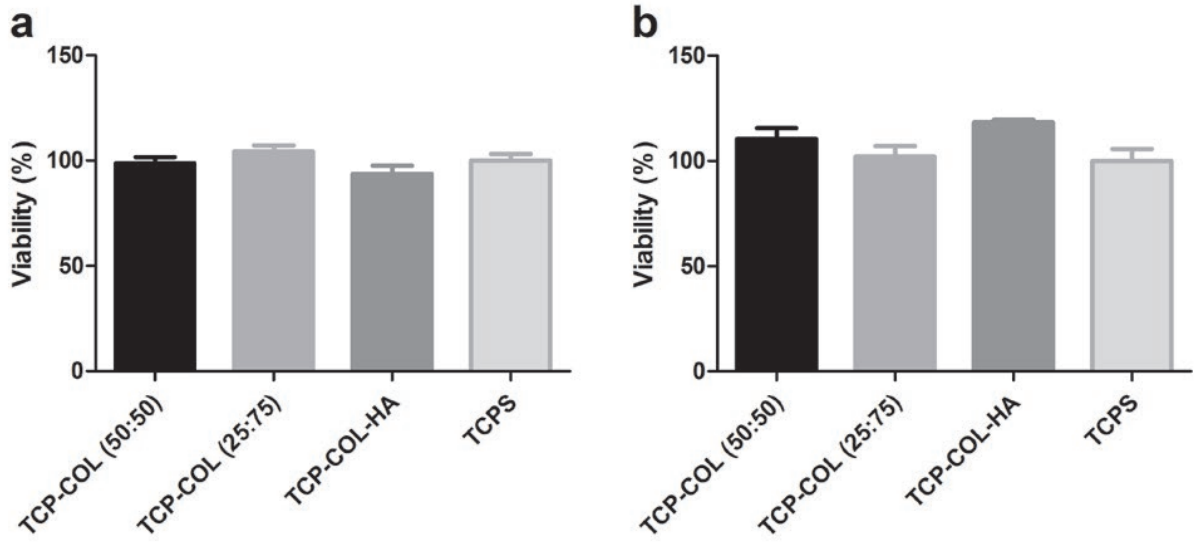

Fig. 3. Cytotoxicity of various scaffolds was assessed using CCK-8. The viability of rMSCs seeded on TCP-COL-HA, TCP-COL (50:50) and TCP-COL (25:75) scaffolds and on 24-well tissue culture polystyrene plates was evaluated at 3 and 7 d. Data are expressed as mean ± SE of three experiments. *$p < 0.05$.

Evaluation of scaffold cytotoxicity

There was no difference in cell viability between the control, TCP-COL (50:50), TCP-COL (25:75), and TCP-COL-HA groups at 3 and 7 d (Fig. 3), indicating that the scaffolds were not toxic to rMSCs.

Characterisation of rMSC-seeded scaffolds

In terms of gross morphology, the TCP-COL-HA scaffold without cells has a rough and porous appearance (Fig. 3a), while the rMSC-seeded TCP-COL-HA scaffold had a smoother and glistening appearance after 3 weeks culture *in vitro* (Fig. 3d). There are no significant differences in appearance between TCP-COL (50:50) and rMSC-seeded TCP-COL (25:75) scaffolds (Fig. 3b, c). The appearances of both rMSC-seeded TCP-COL (50:50) and TCP-COL (25:75) are not as lustrous as that of rMSC-seeded TCP-COL-HA after 3 weeks of culture (Fig. 3b, c and d). An SEM analysis revealed that the TCP-COL-HA scaffold was highly porous, with an interconnected honeycomb-like structure (Fig. 4e, g) and pore sizes of around 50-200 µm that were suitable for rMSC culture. rMSCs were anchored and evenly distributed on the surface of the scaffold at a high density after 3 d of culture (Fig. 4f), and ECM secreted by rMSCs was clearly discernible after 3 weeks of culture (Fig. 4h), indicating that the scaffold had good biocompatibility.

Chondrogenic gene expression analysis

The expression of chondrogenic differentiation markers, including *Aggrecan* and *COL II, X* and *I,* was analysed 3 weeks after induction by qRT-PCR. At 3 weeks, cells in the TCP-COL-HA group had significantly higher expression of *COL II, Aggrecan* and *SOX9* than those in the TCP-COL (25:75) or TCP-COL (50:50) groups, with the latter having the lowest expression (Fig. 5). In contrast, cells in the TCP-COL (50:50) group showed the highest levels of *COL I* and *COL X* at 3 weeks (Fig. 5). Taken together, these results indicate that TCP-COL-HA is more efficient at inducing rMSCs chondrogenic differentiation, whereas TCP-COL (50:50) is more efficient at inducing rMSCs osteogenic/hypertrophic differentiation *in vitro*.

Histological, immunohistochemical and biochemical analyses

H&E staining was carried out to detect differences in the ECM secreted by rMSCs during differentiation. rMSCs were integrated into all three scaffolds at 3 weeks. However, ECM secretion was enhanced in cells seeded on TCP-COL-HA as compared to those grown on scaffolds lacking HA; between the latter two, cells seeded on TCP-COL (25:75) secreted more ECM than those grown on TCP-COL (50:50) at 3 weeks (Fig. 6a).

Alcian blue staining and collagen type II immunohistochemistry at 3 weeks provided evidence for chondrogenic differentiation *in vitro* (Fig. 6b, c). Cells seeded on TCP-COL-HA showed higher collagen type II immunoreactivity than those grown on non-HA scaffolds, with more collagen type II-positive cells observed on the TCP-COL (25:75) than on the TCP-COL (50:50) scaffold at 3 weeks. Similar results were obtained by alcian blue staining. The ratio of IOD *per* stained area for alcian blue staining and collagen type II immunoreactivity at 3 weeks revealed higher levels of GAG and collagen type II in the TCP-COL-HA than in the TCP-COL (25:75) or TCP-COL-HA (50:50) groups, with higher levels observed in the TCP-COL (25:75) than in the TCP-COL (50:50) group (Fig. 6d, e). At 3 weeks, rMSCs seeded on TCP-COL-HA exhibited increased GAG production normalised to dsDNA (GAG/dsDNA) than cells grown on TCP-COL (25:75) or TCP-COL (50:50), with the former producing more GAG/dsDNA than the latter (Fig. 6f). These observations are consistent with results of the qRT-PCR analysis,

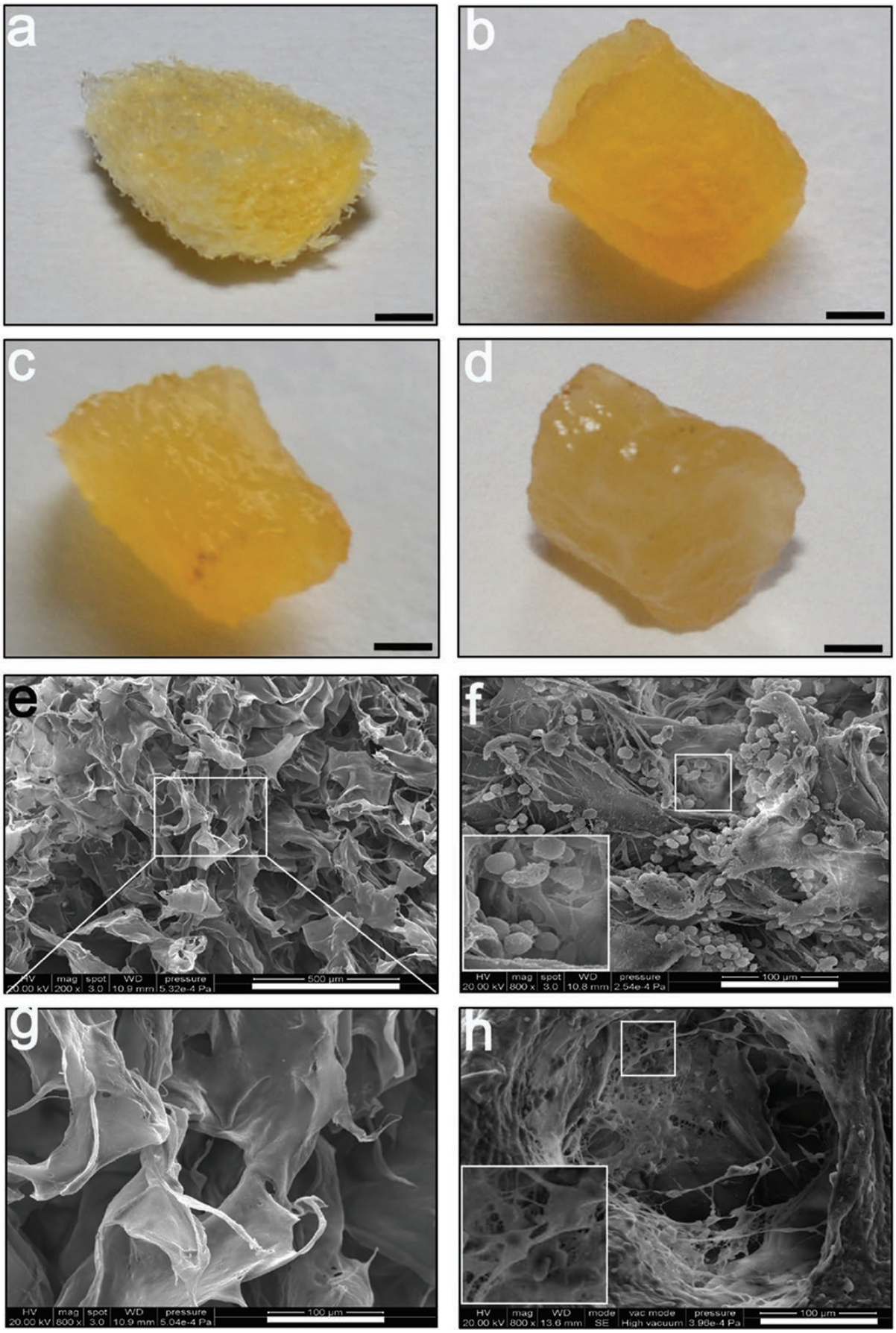

Fig. 4. Gross examination and SEM analysis of rMSC-seeded scaffolds. (**a**, **d**) Images of TCP-COL-HA scaffold without cells (**a**) or seeded with rMSCs after 3 weeks culture (**d**). (**b**, **c**, **e**, **f**) Representative micrographs of the TCP-COL-HA scaffold without cells (**b**, **c**) or seeded with rMSCs after 3 d (**e**) and 3 weeks (**f**) of culture. Images were acquired by SEM (200× and 800×). Scale bar = 2 mm (**a**, **b**, **c**, **d**), 500 µm (**e**), 100 µm (**f**, **g**, **h**).

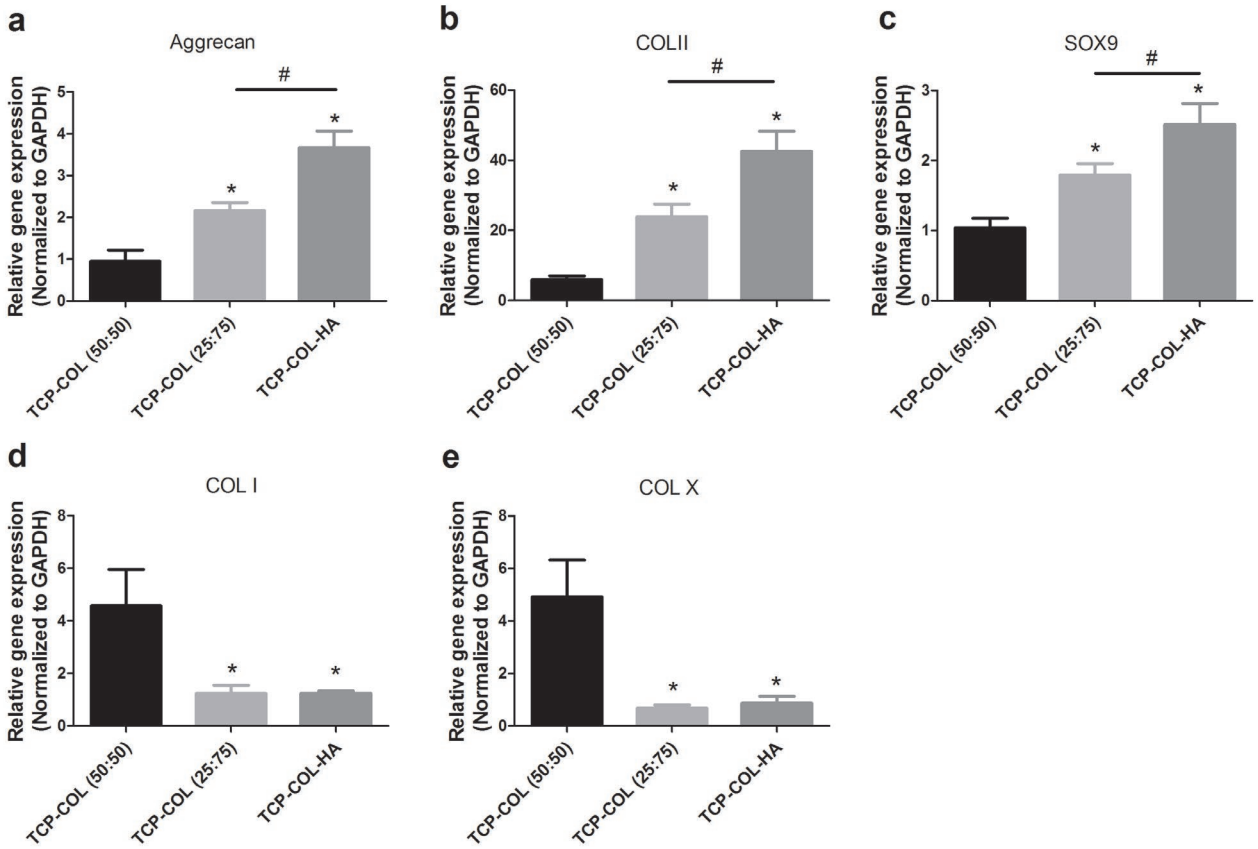

Fig. 5. qRT-PCR analyses of rMSC-seeded scaffolds. Transcript expression of *aggrecan* (**a**), *COL II* (**b**), *SOX9* (**c**), *COL I* (**d**) and *COL X* (**e**) in rMSC-seeded TCP-COL-HA, TCP-COL (25:75) and TCP-COL (50:50) scaffolds, as determined by qRT-PCR after 1, 2 and 3 weeks of culture. Gene expression levels were normalised to that of glyceraldehyde 3-phosphate dehydrogenase (GAPDH). Data represent mean ± SE of three experiments. Within a given group, significant differences ($p < 0.05$) *vs*. TCP-COL (50:50) are denoted by (*) and those between TCP-COL-HA and TCP-COL (25:75) are denoted by (#).

indicating that TCP-COL-HA is more efficient at inducing chondrogenic differentiation of rMSCs *in vitro*.

Analysis of mechanical properties

Mechanical properties of rMSCs were analysed after 3 weeks of culture. The compressive modulus was higher in the TCP-COL-HA than in the TCP-COL (50:50) and TCP-COL (25:75) groups, with no significant difference observed between the latter two (Fig. 7).

Gross observation and histological, immunohistochemical, and biochemical analyses in ectopic cartilage formation assay

The regeneration efficiency of the different scaffolds was compared in an ectopic cartilage regeneration model 4 weeks after implantation. The newly formed tissue-engineered cartilages showed smooth and glistening appearances, and there were no significant differences between the three groups (Fig. 8a, b). H&E and alcian blue staining and collagen type II immunoreactivity were stronger in the TCP-COL-HA than in the TCP-COL groups (Fig. 8c-e), in which staining was more intense for the (25:75) than for the (50:50) group. These results indicate that TCP-COL-HA is the most effective substrate for promoting chondrogenesis and facilitates the secretion of chondrogenic ECM following *in vivo* subcutaneous implantation. A histomorphometric analysis confirmed that GAG and collagen type II were present at the highest levels in the TCP-COL-HA group, followed by the TCP-COL (25:75) and TCP-COL (50:50) (Fig. 8f, g) groups. Moreover, cells seeded on the TCP-COL-HA scaffold had the highest GAG/dsDNA, which was higher in cells grown on TCP-COL (25:75) than on TCP-COL (50:50) (Fig. 8h).

Chondrogenic gene expression analysis in osteochondral repair

The expression of the *Aggrecan*, *COL II*, *SOX9*, *COL I* and *X* were examined 8 weeks after scaffold implantation. The highest levels of gene expression were observed in the TCP-COL-HA group, followed by the TCP-COL (25:50) and TCP-COL (50:50) groups (Fig. 9a-c). On the other hand, the TCP-COL (50:50) group showed higher expression of *COL I* and *X* (Fig. 9d, e).

Gross morphological and histological analyses of osteochondral repair *in vivo*

In untreated control animals, the osteochondral defect was nearly devoid of tissue after 8 weeks, with only amorphous soft fibres observed in the central area (Fig. 10a) and a chondral phase that was completely denuded

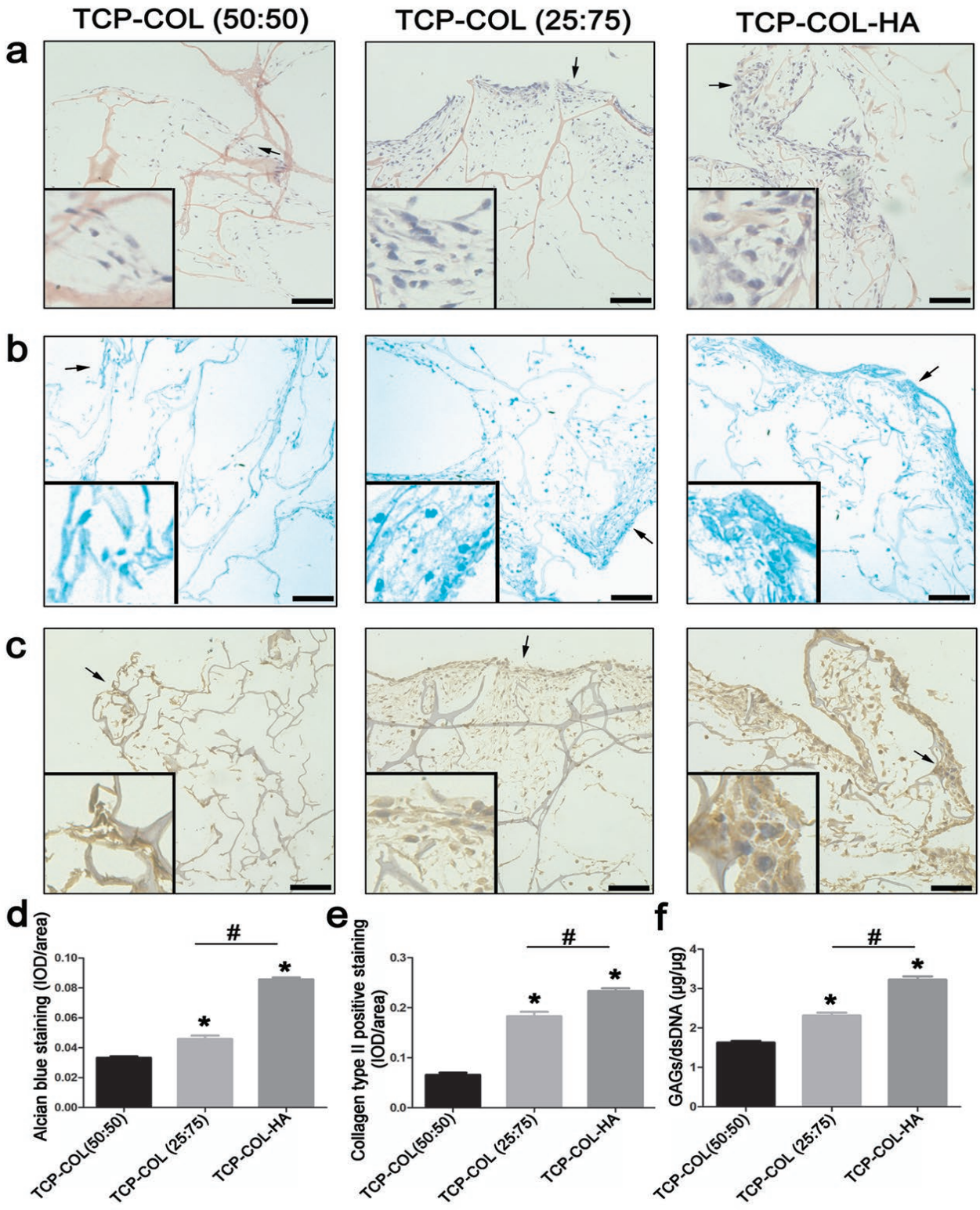

Fig. 6. Histomorphometric and biochemical analyses of rMSC-seeded scaffolds. (**a-c**) Histological characteristics were examined by H&E staining (**a**), alcian blue staining (**b**) and collagen type II immunohistochemistry (**c**). (**d**, **e**) Average IOD/area for alcian blue staining (**d**) and collagen type II immunohistochemistry (**e**) of rMSC-seeded scaffolds after 3 weeks of culture. (**f**) Quantification of GAGs/dsDNA in rMSCs seeded on scaffolds at 1, 2 and 3 weeks. Data represent mean ± SE of three experiments. Within a given group, significant differences ($p < 0.05$) *vs*. TCP-COL (50:50) are denoted by (*), and those between TCP-COL-HA and TCP-COL (25:75) are denoted by (#). Scale bar = 100 μm. IOD/area, integrated optical density *per* stained area.

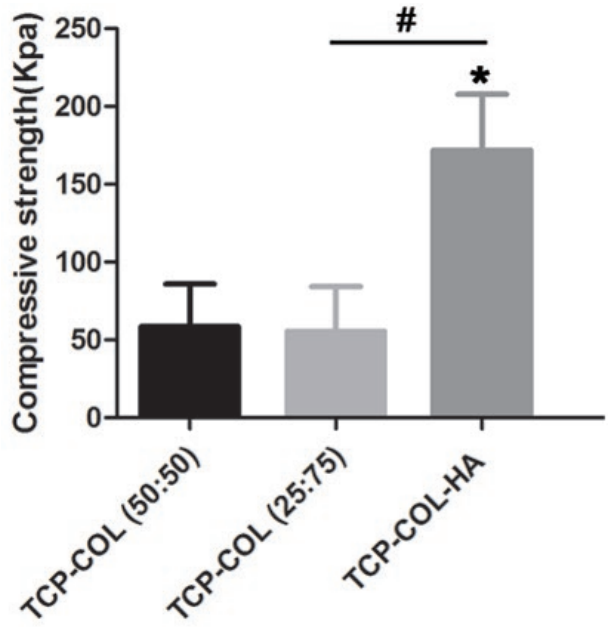

Fig. 7. Analysis of mechanical properties of rMSC-seeded scaffolds. Mechanical properties were evaluated 4 weeks after seeding with rMSCs. Data represent mean ± SE of three experiments. *$p < 0.05$.

(Fig. 10e, i, m). H&E, alcian blue and safranin O staining revealed only small amounts of newly formed cartilage in the chondral region, suggesting limited intrinsic repair capability. Marginal tissue repair was detected in the TCP-COL (50:50) group; most of the regenerated tissue within the defect was thin and rough, and some scaffold remained within the centre, although it had mostly integrated into adjacent host cartilage (Fig. 10b). The defect was filled with loose regenerated tissue and the cell-seeded scaffold. Only small areas of the defect were positive for alcian blue and safranin O staining (Fig. 10f, j, n). In the TCP-COL (25:75) group, the regenerated tissue was thicker and its surface topography was more similar to that of host cartilage, although the junction between the two was still identifiable and alcian blue and safranin O staining intensity was weaker than in native cartilage (Fig. 10c, g, k, o). Numerous chondrocyte-like cells surrounded by dense ECM were observed within the defect (Fig. 10s). Meanwhile, in the TCP-COL-HA group, the regenerated tissue completely occupied the defect and had a glistening white appearance, with only a pinhole remaining in the central area (Fig. 10d). The regenerated tissue was similar in colour and texture to native cartilage, as evidence by strong alcian blue and safranin O staining for GAG (Fig. 10h, l, p). At higher magnification, the integration of the regenerated tissue into native cartilage was greater in TCP-COL-HA and TCP-COL (25:75) than in the other two groups (Fig. 10q-t), while the TCP-COL (50:50) was superior to the untreated control group. A histomorphometric analysis revealed that GAG levels were highest in the TCP-COL-HA group, followed by those in the TCP-COL (25:75) and TCP-COL (50:50) groups and untreated controls (Fig. 10u, v).

Biochemical assay for GAGs in osteochondral repair

The GAG/dsDNA ratio is indicative of the quality of regenerated cartilage. The ratio was highest in the TCP-COL-HA group, followed by the TCP-COL (25:75) and TCP-COL (50:50) groups (Fig. 10w).

Discussion

In this study, we found that the TCP-COL-HA scaffold can function as a stem cell carrier to induce chondrogenesis of rMSCs *in vitro* and *in vivo* and thereby promote cartilage repair in rabbits. The TCP-COL-HA scaffold showed more cartilaginous characteristics than the TCP-COL scaffold. Of the latter, TCP-COL (25:75) was superior to TCP-COL (50:50) in terms of inducing chondrogenic differentiation of rMSCs and repairing cartilage defect.

Application of chondrogenic growth factors, especially TGF-β, is a routine strategy for inducing chondrogenesis of hMSCs, but they have safety problems in the long term. Scaffolding material has always been expected to play a crucial role in inducting chondrogenic differentiation of MSCs to generate cartilage tissue. We previously demonstrated that the TCP-COL-HA scaffold can induce chondrogenic differentiation of both ATDC5 and hMSCs without TGF-β *in vitro* (Meng *et al*., 2014). In this study, we found that the TCP-COL-HA scaffold can induce chondrogenesis of rMSCs *in vitro* and *in vivo* and have good potential for cartilage repair. Similar results have been reported in previous studies using other materials. A natural scaffold composed of ECM produced by chondrocytes was successfully used to promote chondrogenic differentiation of rMSCs without TGF-β treatment (Choi *et al*., 2010). Gelatin-chitosan hybrid materials have been reported to increase ECM synthesis and promote MSC chondrogenesis (Breyner *et al*., 2010). However, conflicting results were reported by other investigators using TGF-β3 and HA in a photopolymerised hydrogel; in this case, TGF-β3 was demonstrated to be essential for proteoglycan production (Sharma *et al*., 2007). The discrepancy in the results may be attributable to the HA and materials, which were different from those used in the present study. For instance, the previous study used an HA with a molecular weight of 1.1×10^6 Da, while the one used here was 2×10^6 Da. Previous studies have found that HA molecules of 1.65-3×10^6 Da can induce chondrogenic differentiation of rMSCs (Hegewald *et al*., 2004). Overall, these results suggest that the growth factors may not be critical if optimal conditions for chondrogenic differentiation of MSCs are provided by scaffolds. Inducing chondrogenic differentiation of MSCs, without the need for biological factor(s), would be beneficial in terms of avoiding potentially harmful effects and reducing production costs for therapy.

HA can promote chondrogenic differentiation of MSCs in TCP-COL-HA scaffolds. The qPCR, GAG/dsDNA, alcian blue staining and collagen type II immunohistochemical staining results (Figs.5, 6, 8-10) indicate that the scaffold containing HA more efficiently induced chondrogenic differentiation of rMSCs *in vitro*

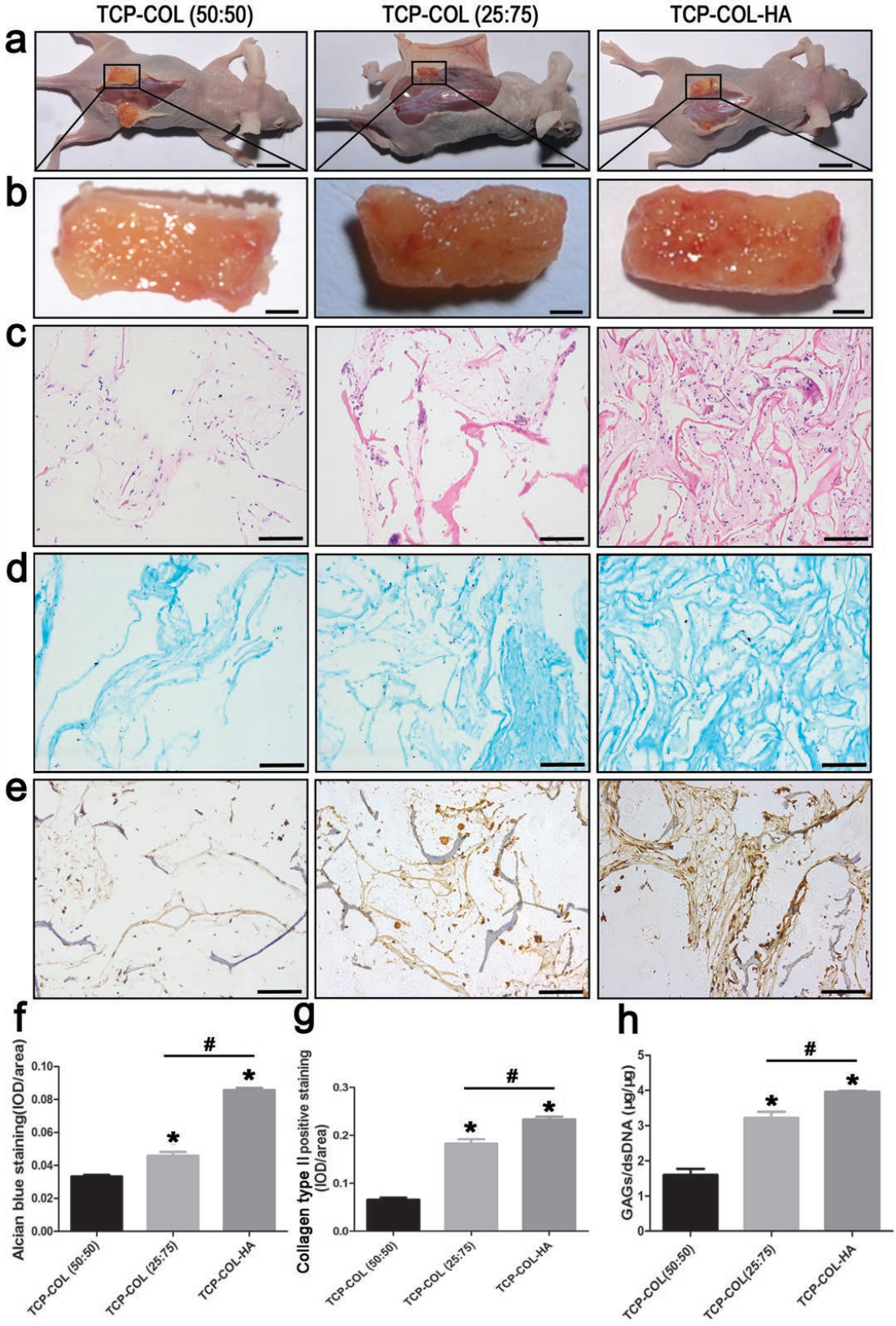

Fig. 8. Efficiency of ectopic cartilage regeneration by rMSC-seeded scaffolds *in vivo*. (**a**-**e**) TCP-COL-HA, TCP-COL (25:75) and TCP-COL (50:50) scaffolds seeded with rMSCs were subcutaneously implanted into the backs of nude mice, and their morphology and histological characteristics were assessed 4 weeks later by gross examination (**a**, **b**), H&E staining (**c**), alcian blue staining (**d**) and immunohistochemical analysis of collagen type II expression (**e**). (**f**, **g**) Average IOD/area for alcian blue staining (**f**) and collagen type II immunohistochemistry (**g**) of rMSCs seeded on scaffolds. (**h**) Quantification of GAGs/dsDNA in rMSCs seeded on scaffolds 4 weeks after implantation into nude mice. Data represent mean ± SE of three experiments. Within a given group, significant differences ($p < 0.05$) *vs*. TCP-COL (50:50) are denoted by (*); those between TCP-COL-HA and TCP-COL (25:75) are denoted by (#). Scale bar = 1 cm (**a**), 1 mm (**b**), 100 μm (**c**, **d**, **e**). IOD/area, integrated optical density *per* stained area.

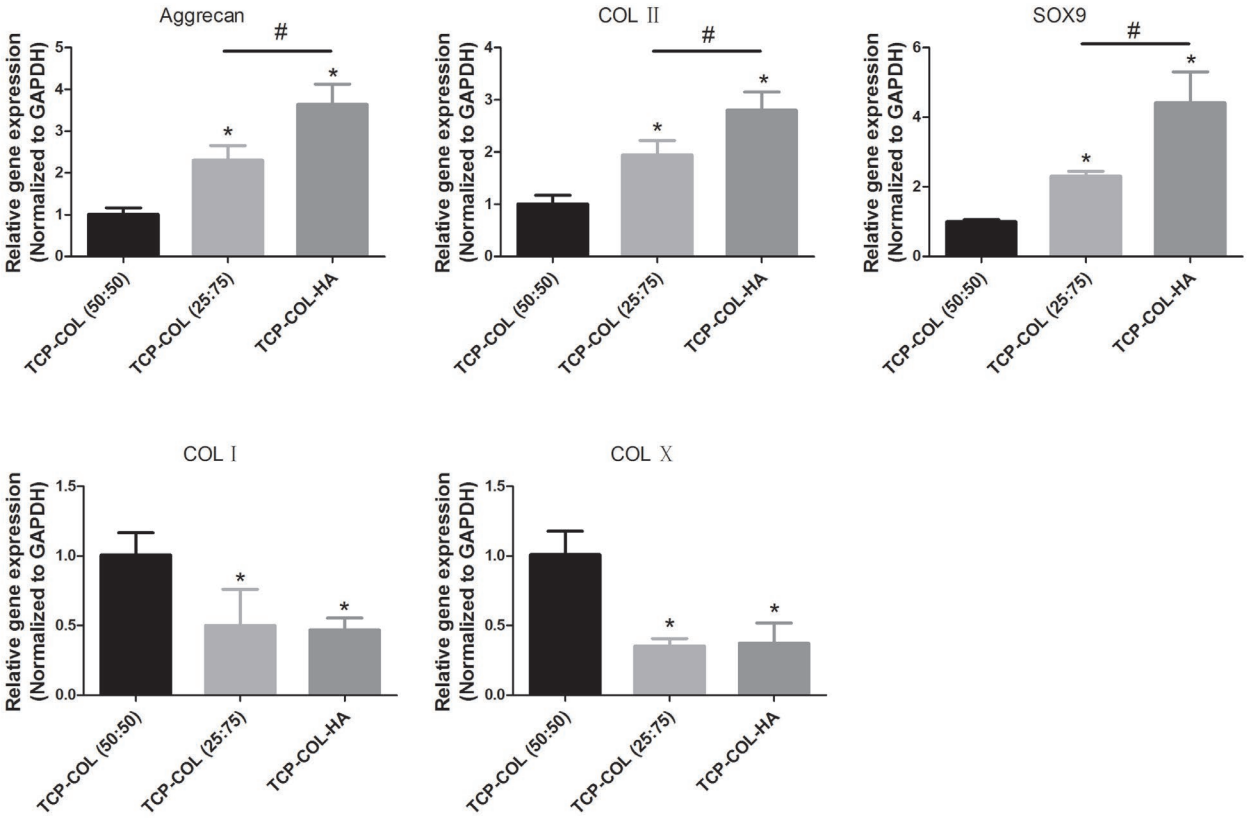

Fig. 9. Analysis of marker gene expression in implanted rMSC-seeded scaffolds. Transcript levels of (**a**) *aggrecan*, (**b**) *COL II*, (**c**) *SOX9*, (**d**) *COL I* and (**e**) *COL X* in rMSCs seeded on TCP-COL-HA, TCP-COL (25:75) and TCP-COL (50:50) scaffolds were measured by qRT-PCR 8 weeks after implantation into osteochondral defects of rabbits. Data represent mean ± SE of three experiments. Within a given group, significant differences ($p < 0.05$) *vs*. TCP-COL (50:50) are denoted by (*); those between TCP-COL-HA and TCP-COL (25:75) are denoted by (#).

and *in vivo*, and resulted in regenerated tissue of higher quality than those without HA, consistent with several other HA-based culture models (Park and Lee, 2014; Schagemann *et al*., 2013). One study found that HA added to human MSCs in alginate increased cartilage matrix production (Kavalkovich *et al*., 2002), suggesting a direct biological role for this molecule. The reason for enhanced chondrogenic differentiation by inclusion of HA in the scaffold is unclear, but may involve signal transduction pathways that are modulated by interactions between rMSCs and the ECM environment of TCP-COL-HA. HA interacts with the transmembrane receptor CD44 (Knudson and Loeser, 2002; Park and Lee, 2014), which mediates cell adhesion, growth and differentiation (Ishida *et al*., 1996; Maleski and Knudson, 1996); in the present study, before seeding on scaffolds, about 97.42 % of rMSCs were positive for CD44 expression.

TCP/COL ratio may affect the chondro-inductive capacity of scaffolds. Previous studies have demonstrated that both TCP and COL scaffolds support the repair of osteochondral defects (Dawson *et al*., 2008; Stark *et al*., 2006; Tanaka *et al*., 2005). However, there are few studies comparing the effects of different ratios of TCP to COL in hybrid scaffolds. Our study found TCP-COL (25:75) more effectively induced chondrogenic differentiation of rMSCs *in vitro* and *in vivo* as compared to TCP-COL (50:50). In contrast, TCP-COL (50:50) more effectively induced hypertrophy during the chondrogenic differentiation of rMSCs. Two mechanisms are proposed to account for this observation. Firstly, some studies have shown that type I COL hydrogels can induce chondrogenesis *in vitro* (Zhang *et al*., 2012) and *in vivo* (Kuroda *et al*., 2007; Zheng *et al*., 2009). Secondly, TCP-containing materials have the potential to increase calcium concentration outside of MSCs, which is critical for mineralisation of osteoblast-like cells (Chang *et al*., 2000; Matsuoka *et al*., 1999), which likely contributes to hypertrophy during chondrogenic differentiation of rMSCs.

The mechanical integrity of a scaffold plays an important role in its effectiveness as a biomaterial. COL products have inadequate mechanical properties, which are important for tissues that are continuously subjected to compressive forces *in vivo* (Bakoš *et al*., 1999). The addition of TCP enhances the mechanical properties of COL scaffolds (Arahira and Todo, 2014); as such, it is important to compare materials with different TCP/COL ratios to determine the ideal balance between chondrogenesis-inducing capability and good mechanical properties. In our study, the TCP-COL (25:75) scaffold promoted cartilage formation to a greater degree than the TCP-COL (50:50) scaffold; however, there was no significant difference in the mechanical strength after 3 weeks culture *in vitro* between the two types of scaffold seeded with rMSCs. This may be due to increased ECM, GAGs and type II COL formation

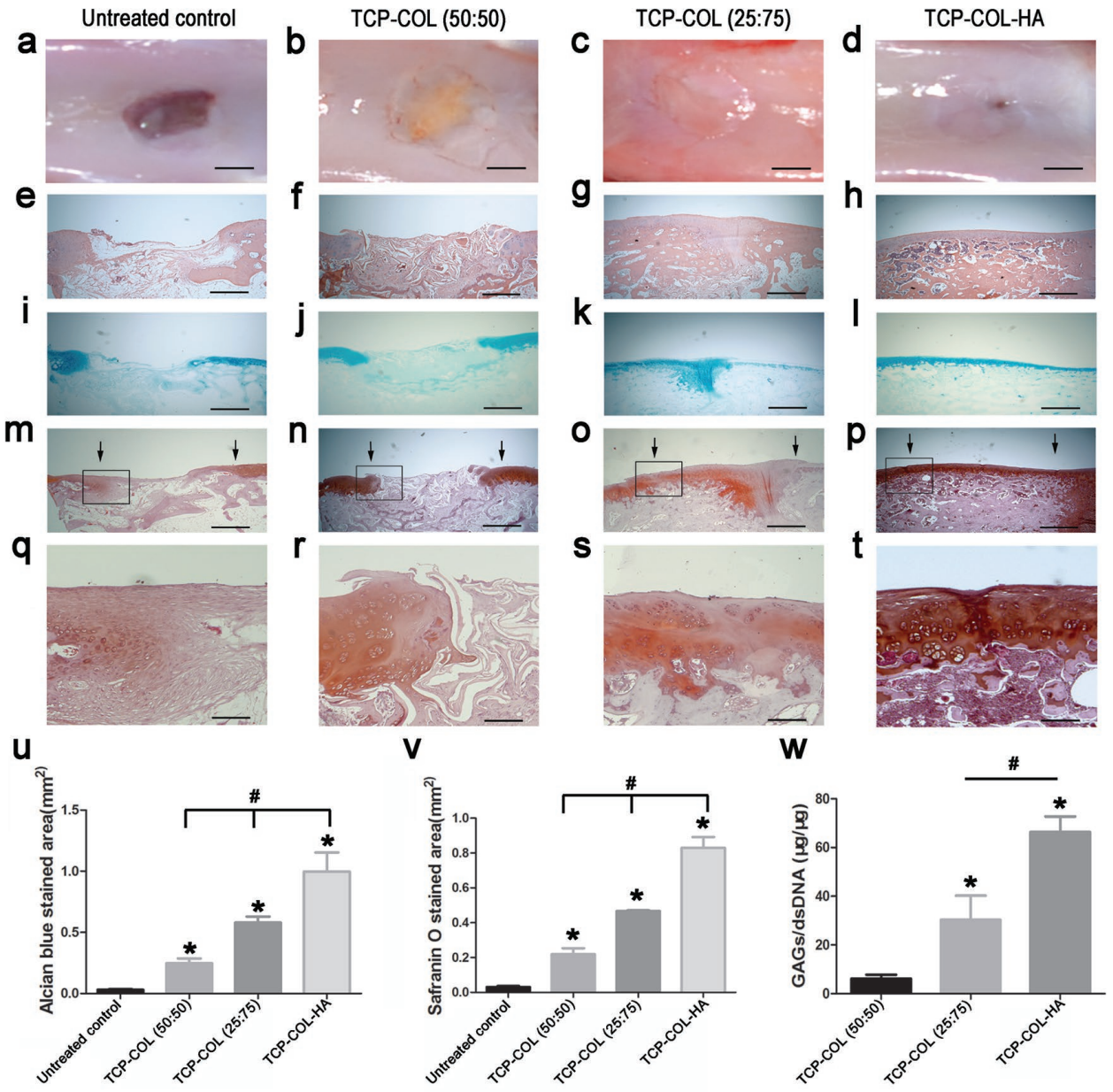

Fig. 10. Evaluation of rabbit osteochondral defect repair 8 weeks after scaffold implantation. (**a-d**) Gross appearance of defects in the untreated control (**a**), TCP-COL (50:50) (**b**), TCP-COL (25:75) (**c**) and TCP-COL-HA (**d**) groups. (**e-p**) Tissue specimens were stained with H&E (**e-h**), alcian blue (**i-l**) and safranin O (**m-p**). (**q-t**) Magnified view of areas enclosed by black boxes in (**m-p**). (**u**, **v**) Histomorphometric analyses of areas stained with alcian blue (**u**) and safranin O (**v**). (**w**) Quantification of GAGs/dsDNA in rMSCs seeded on scaffolds 8 weeks after implantation. Data represent mean ± standard error of three experiments. Within a given group, significant differences ($p < 0.05$) *vs*. TCP-COL (50:50) are denoted by (*); those between TCP-COL-HA and TCP-COL (25:75) are denoted by (#). Scale bar = 1 mm (**a-p**), 200 μm (**q-t**).

(Fig. 6), which have been shown to increase the mechanical strength of scaffolds (Tigli *et al*., 2011; Williamson *et al*., 2001; Wilson *et al*., 2007). The TCP-COL-HA (25:73:2) scaffold had the highest compressive modulus among all substrates tested in our study. This may be due to the presence of HA; it was previously shown that 2 % HA enhanced the mechanical properties of tissue-engineered cartilage constructs (Levett *et al*., 2014), and that addition of exogenous high molecular weight HA to cell-seeded COL gels increased tensile strength (Allison *et al*., 2009). Further studies are needed to clarify the exact relationship between HA in the mechanical properties of scaffolds.

The present study had limitations. We implanted rMSC-seeded scaffolds subcutaneously into nude mice and assessed chondrogenesis after four weeks only, but not eight. Although a longer subcutaneous implantation period in nude mice may be better for evaluating long-term effects, a four-week subcutaneous implantation time has been widely used in recent cartilage tissue regeneration studies (Dawson *et al*., 2008; Bae *et al*., 2010; Jung *et al*., 2010; Pelttari *et al*., 2006; Xue *et al*., 2012). Another limitation is that the effect of host tissue

carryover during harvesting on qPCR and GAG/dsDNA data for subcutaneous and osteochondral samples may exist. The nude mice subcutaneous implantation model and rabbit osteochondral defect models have been widely used for various purposes in cartilage tissue engineering research (De Bari *et al*., 2004; Kim *et al*., 2011; Lam *et al*., 2014; Liu *et al*., 2011; Pelttari *et al*., 2006). In our study, certain prevention measures have been taken to control for the effect of host tissue carryover. For the subcutaneous and osteochondral samples, host tissues were carefully removed using fine, straight, toothless forceps, small curved, toothless forceps, #15 blade in #3 handle under a stereoscope (10× magnification) from the implanted samples to limit the presence of host tissues in our samples. For biochemical assays and qRT-PCR, we mainly harvested the sample from the middle of the regenerative tissue, to avoid getting marginal parts (the integration part of the regenerated tissue into native tissue) in order to prevent the presence of host tissues in our samples.

In our next study, we will use more control scaffolds (*e.g*., COL-HA, COL, HA, TCP, TCP-HA and TCP-COL scaffolds in various ratios) to examine in greater detail the mechanism of the TCPCOL-HA scaffold in inducing chondrogenic differentiation of MSCs in order to further improve its effectiveness. Additionally, we are also considering using the TCP-COL-HA biomaterials in an intraoperative setup that circumvents the need for cell expansion so that the scaffold can, for example, be used in combination with marrow stimulation techniques, which are regularly used in clinics and would enhance the translational potential of the scaffold.

Conclusion

In conclusion, TCP-COL-HA induced the chondrogenesis of rMSCs and facilitated the repair of osteochondral defects. The addition of HA and different TCP/COL ratios affected the chondro-inductive effects of the scaffold. These findings suggest that the novel TCP-COL-HA scaffold might help to improve cartilage tissue engineering with safety and economic benefit, and be worthy of further investigation towards aimed clinical applications.

Acknowledgments

We thank Gang Wu (South China University of Technology, Guangzhou, China) for providing scaffold materials and technical assistance. This work was supported by the National Nature Science Foundation of China (81572119 & 81472101), and the Guangdong Provincial Natural Science Foundation of China (2014A030313064 & 2014A030313186). We confirm that the authors have no conflicts of interest to declare and there has been no significant financial support for this work that could influence its outcome.

References

Ahn J, Lee T, Oh J, Kim S, Kim H, Park I, Choi B, Im G (2009) A novel hyaluronate-atelocollagen/β-TCP-hydroxyapatite biphasic scaffold for the repair of osteochondral defects in rabbits. Tissue Eng Part A **15:** 2595-2604.

Allison DD, Braun KR, Wight TN, Grande-Allen KJ (2009) Differential effects of exogenous and endogenous hyaluronan on contraction and strength of collagen gels. Acta Biomater **5:** 1019-1026.

Arahira T, Todo M (2014) Effects of proliferation and differentiation of mesenchymal stem cells on compressive mechanical behavior of collagen/beta-TCP composite scaffold. J Mech Behav Biomed Mater **39:** 218-230.

Bae SE, Choi DH, Han DK, Park K (2010) Effect of temporally controlled release of dexamethasone on *in vivo* chondrogenic differentiation of mesenchymal stromal cells. J Control Release **143:** 23-30.

Bakoš D, Soldán M, Hernández-Fuentes I (1999) Hydroxyapatite-collagen-hyaluronic acid composite. Biomaterials **20:** 191-195.

Breyner NM, Hell RC, Carvalho LR, Machado CB, Peixoto FI, Valerio P, Pereira MM, Goes AM (2010) Effect of a three-dimensional chitosan porous scaffold on the differentiation of mesenchymal stem cells into chondrocytes. Cells Tissues Organs **191:** 119-128.

Caplan AI (2005) Review: mesenchymal stem cells: cell-based reconstructive therapy in orthopedics. Tissue Eng **11:** 1198-1211.

Chang YL, Stanford CM, Keller JC (2000) Calcium and phosphate supplementation promotes bone cell mineralization: implications for hydroxyapatite (HA)-enhanced bone formation. J Biomed Mater Res **52:** 270-278.

Chen H, Sun J, Hoemann CD, Lascau-Coman V, Ouyang W, McKee MD, Shive MS, Buschmann MD (2009) Drilling and microfracture lead to different bone structure and necrosis during bone-marrow stimulation for cartilage repair. J Orthop Res **27:** 1432-1438.

Choi KH, Choi BH, Park SR, Kim BJ, Min BH (2010) The chondrogenic differentiation of mesenchymal stem cells on an extracellular matrix scaffold derived from porcine chondrocytes. Biomaterials **31:** 5355-5365.

Curran JM, Chen R, Hunt JA (2006) The guidance of human mesenchymal stem cell differentiation *in vitro* by controlled modifications to the cell substrate. Biomaterials **27:** 4783-4793.

Dawson JI, Wahl DA, Lanham SA, Kanczler JM, Czernuszka JT, Oreffo RO (2008) Development of specific collagen scaffolds to support the osteogenic and chondrogenic differentiation of human bone marrow stromal cells. Biomaterials **29:** 3105-3116.

De Bari C, Dell'Accio F, Luyten FP (2004) Failure of *in vitro*-differentiated mesenchymal stem cells from the synovial membrane to form ectopic stable cartilage *in vivo*. Arthritis Rheum **50:** 142-150.

Glowacki J, Mizuno S (2008) Collagen scaffolds for tissue engineering. Biopolymers **89:** 338-344.

Goodstone NJ, Cartwright A, Ashton B (2004) Effects of high molecular weight hyaluronan on chondrocytes

cultured within a resorbable gelatin sponge. Tissue Eng **10:** 621-631.

Gotterbarm T, Richter W, Jung M, Berardi VS, Mainil-Varlet P, Yamashita T, Breusch SJ (2006) An *in vivo* study of a growth-factor enhanced, cell free, two-layered collagen-tricalcium phosphate in deep osteochondral defects. Biomaterials **27:** 3387-3395.

Hegewald AA, Ringe J, Bartel J, Krüger I, Notter M, Barnewitz D, Kaps C, Sittinger M (2004) Hyaluronic acid and autologous synovial fluid induce chondrogenic differentiation of equine mesenchymal stem cells: a preliminary study. Tissue Cell **36:** 431-438.

Hubbell JA (2003) Materials as morphogenetic guides in tissue engineering. Curr Opin Biotechnol **14:** 551-558.

Hunziker EB (2002) Articular cartilage repair: basic science and clinical progress. A review of the current status and prospects. Osteoarthritis Cartilage **10:** 432-463.

Ishida T, Iijima T, Moriyama S, Nakamura C, Kitagawa T, Machinami R (1996) Intra-articular calcifying synovial sarcoma mimicking synovial chondromatosis. Skeletal Radiol **25:** 766-769.

Jackson DW, Simon TM (1999) Tissue engineering principles in orthopaedic surgery. Clin Orthop Relat Res **367 Suppl:** S31-45.

Johnstone B, Hering TM, Caplan AI, Goldberg VM, Yoo JU (1998) *In vitro* chondrogenesis of bone marrow-derived mesenchymal progenitor cells. Exp Cell Res **238:** 265-272.

Jung HH, Park K, Han DK (2010) Preparation of TGF-beta1-conjugated biodegradable pluronic F127 hydrogel and its application with adipose-derived stem cells. J Control Release **147:** 84-91.

Kavalkovich KW, Boynton RE, Murphy JM, Barry F (2002) Chondrogenic differentiation of human mesenchymal stem cells within an alginate layer culture system. In Vitro Cell Dev Biol Anim **38:** 457-466.

Kim M, Kim SE, Kang SS, Kim YH, Tae G (2011) The use of de-differentiated chondrocytes delivered by a heparin-based hydrogel to regenerate cartilage in partial-thickness defects. Biomaterials **32:** 7883-7896.

Knudson W, Loeser RF (2002) CD44 and integrin matrix receptors participate in cartilage homeostasis. Cell Mol Life Sci **59:** 36-44.

Kuroda R, Ishida K, Matsumoto T, Akisue T, Fujioka H, Mizuno K, Ohgushi H, Wakitani S, Kurosaka M (2007) Treatment of a full-thickness articular cartilage defect in the femoral condyle of an athlete with autologous bone-marrow stromal cells. Osteoarthritis Cartilage **15:** 226-231.

Lam J, Lu S, Lee EJ, Trachtenberg JE, Meretoja VV, Dahlin RL, van den Beucken JJ, Tabata Y, Wong ME, Jansen JA, Mikos AG, Kasper FK (2014) Osteochondral defect repair using bilayered hydrogels encapsulating both chondrogenically and osteogenically pre-differentiated mesenchymal stem cells in a rabbit model. Osteoarthritis Cartilage **22:** 1291-1300

Langer R, Vacanti JP (1993) Tissue engineering. Science **260:** 920-926.

Levett PA, Hutmacher DW, Malda J, Klein TJ (2014) Hyaluronic acid enhances the mechanical properties of tissue-engineered cartilage constructs. PLoS One **9:** e113216.

Liu X, Jin X, Ma PX (2011) Nanofibrous hollow microspheres self-assembled from star-shaped polymers as injectable cell carriers for knee repair. Nat Mater **10:** 398-406.

Maleski MP, Knudson CB (1996) Matrix accumulation and retention in embryonic cartilage and *in vitro* chondrogenesis. Connect Tissue Res **34:** 75-86.

Marquass B, Somerson JS, Hepp P, Aigner T, Schwan S, Bader A, Josten C, Zscharnack M, Schulz RM (2010) A novel MSC-seeded triphasic construct for the repair of osteochondral defects. J Orthop Res **28:** 1586-1599.

Matsuoka H, Akiyama H, Okada Y, Ito H, Shigeno C, Konishi J, Kokubo T, Nakamura T (1999) *In vitro* analysis of the stimulation of bone formation by highly bioactive apatite- and wollastonite-containing glass-ceramic: released calcium ions promote osteogenic differentiation in osteoblastic ROS17/2.8 cells. J Biomed Mater Res **47:** 176-188.

Meng F, He A, Zhang Z, Zhang Z, Lin Z, Yang Z, Long Y, Wu G, Kang Y, Liao W (2014) Chondrogenic differentiation of ATDC5 and hMSCs could be induced by a novel scaffold-tricalcium phosphate-collagen-hyaluronan without any exogenous growth factors *in vitro*. J Biomed Mater Res A **102:** 2725-2735.

Mueller MB, Fischer M, Zellner J, Berner A, Dienstknecht T, Prantl L, Kujat R, Nerlich M, Tuan RS, Angele P (2010) Hypertrophy in mesenchymal stem cell chondrogenesis: effect of TGF-beta isoforms and chondrogenic conditioning. Cells Tissues Organs **192:** 158-166.

Nettles DL, Vail TP, Morgan MT, Grinstaff M., Setton LA (2004) Photocrosslinkable hyaluronan as a scaffold for articular cartilage repair. Ann Biomed Eng **32:** 391-397.

Park H, Lee KY (2014) Cartilage regeneration using biodegradable oxidized alginate/hyaluronate hydrogels. J Biomed Mat Res **102:** 4519-4525

Park SH. Choi BH, Park SR, Min BH (2011) Chondrogenesis of rabbit mesenchymal stem cells in fibrin/hyaluronan composite scaffold *in vitro*. Tissue Eng Part A **17:** 1277-1286.

Pavesio A, Abatangelo G, Borrione A, Brocchetta D, Hollander AP, Kon E, Torasso F, Zanasi S, Marcacci M (2003) Hyaluronan-based scaffolds (Hyalograft C) in the treatment of knee cartilage defects: preliminary clinical findings. Novartis Found Symp **249:** 203-217.

Pelttari K, Winter A, Steck E, Goetzke K, Hennig T, Ochs BG, Aigner T, Richter W (2006) Premature induction of hypertrophy during *in vitro* chondrogenesis of human mesenchymal stem cells correlates with calcification and vascular invasion after ectopic transplantation in SCID mice. Arthritis Rheum **54:** 3254-3266.

Radice M, Brun P, Cortivo R, Scapinelli R, Battaliard C, Abatangelo G (2000) Hyaluronan-based biopolymers as delivery vehicles for bone-marrow-derived mesenchymal progenitors. J Biomed Mater Res **50:** 101-109.

Revell CM, Athanasiou KA (2009) Success rates and immunologic responses of autogenic, allogenic, and xenogenic treatments to repair articular cartilage defects. Tissue Eng Part B Rev **15:** 1-15.

Schagemann JC, Paul S, Casper ME, Rohwedel J, Kramer J, Kaps C, Mittelstaedt H, Fehr M, Reinholz GG

(2013) Chondrogenic differentiation of bone marrow-derived mesenchymal stromal cells *via* biomimetic and bioactive poly-ε-caprolactone scaffolds. J Biomed Mater Res A **101A:** 1620-1628.

Seo JP, Tanabe T, Tsuzuki N, Haneda S, Yamada K, Furuoka H, Tabata Y, Sasaki N (2013) Effects of bilayer gelatin/beta-tricalcium phosphate sponges loaded with mesenchymal stem cells, chondrocytes, bone morphogenetic protein-2, and platelet rich plasma on osteochondral defects of the talus in horses. Res Vet Sci **95:** 1210-1216.

Sharma B, Williams CG, Khan M, Manson P, Elisseeff JH (2007) *In vivo* chondrogenesis of mesenchymal stem cells in a photopolymerized hydrogel. Plast Reconstr Surg **119:** 112-120.

Solchaga LA, Temenoff JS, Gao J, Mikos AG, Caplan AI, Goldberg VM (2005) Repair of osteochondral defects with hyaluronan- and polyester-based scaffolds. Osteoarthritis Cartilage **13:** 297-309.

Stark Y, Suck K, Kasper C, Wieland M, van Griensven M, Scheper T (2006) Application of collagen matrices for cartilage tissue engineering. Exp Toxicol Pathol **57:** 305-311.

Steadman JR, Rodkey WG, Briggs KK (2002) Microfracture to treat full-thickness chondral defects: surgical technique, rehabilitation, and outcomes. J Knee Surg **15:** 170-176.

Stoop R (2008) Smart biomaterials for tissue engineering of cartilage. Injury **39 Suppl 1:** S77-87.

Tanaka T, Komaki H, Chazono M, Fujii K (2005) Use of a biphasic graft constructed with chondrocytes overlying a β-tricalcium phosphate block in the treatment of rabbit osteochondral defects. Tissue Eng **11:** 331-339.

Tigli RS, Cannizaro C, Gumusderelioglu M, Kaplan DL (2011) Chondrogenesis in perfusion bioreactors using porous silk scaffolds and hESC-derived MSCs. J Biomed Mater Res A **96:** 21-28.

van Beuningen HM, Glansbeek HL, van der Kraan PM, van den Berg WB (1998) Differential effects of local application of BMP-2 or TGF-beta 1 on both articular cartilage composition and osteophyte formation. Osteoarthritis Cartilage **6:** 306-317.

Williamson AK, Chen AC, Sah RL (2001) Compressive properties and function-composition relationships of developing bovine articular cartilage. J Orthop Res **19:** 1113-1121.

Wilson W, Huyghe JM, van Donkelaar CC (2007) Depth-dependent compressive equilibrium properties of articular cartilage explained by its composition. Biomech Model Mechanobiol **6:** 43-53.

Xue JX, Gong YY, Zhou GD, Liu W, Cao Y, Zhang WJ (2012) Chondrogenic differentiation of bone marrow-derived mesenchymal stem cells induced by acellular cartilage sheets. Biomaterials **33:** 5832-5840.

Zhang L, Yuan T, Guo L, Zhang X (2012) An *in vitro* study of collagen hydrogel to induce the chondrogenic differentiation of mesenchymal stem cells. J Biomed Mater Res A. **100A:** 2717-2725.

Zheng L, Sun J, Chen X, Wang G, Jiang B, Fan H, Zhang X (2009) *In vivo* cartilage engineering with collagen hydrogel and allogenous chondrocytes after diffusion chamber implantation in immunocompetent host. Tissue Eng Part A **15:** 2145-2153.

Discussion with Reviewers

Reviewer II: The scaffolds presented seem to have good potential for cartilage repair. Did the authors consider using these biomaterials in an intraoperative setup without need of cell expansion? One possibility could be for example using the scaffold in combination with marrow stimulation techniques, as already performed in the clinics on a regular basis. That would significantly increase the clinical translation significance of the work.

Authors: We completely agree with the reviewer and we have already added this in our discussion in the revised manuscript by stating "Additionally, we are also considering using the TCP-COL-HA biomaterials in an intraoperative setup that circumvents the need for cell expansion so that the scaffold can, for example, be used in combination with marrow stimulation techniques, which are regularly used in clinics and would enhance the translational potential of the scaffold."

Editor's Note: Scientific Editor in charge of the paper: Mauro Alini.